

PAPER • OPEN ACCESS

## Numerical investigation of the effects of hydrofoil vibrations on the unsteady behavior of cavitation

To cite this article: Linlin Geng *et al* 2021 *IOP Conf. Ser.: Earth Environ. Sci.* **774** 012078

View the [article online](#) for updates and enhancements.



**The Electrochemical Society**  
Advancing solid state & electrochemical science & technology

The ECS is seeking candidates to serve as the  
**Founding Editor-in-Chief (EIC) of ECS Sensors Plus,**  
a journal in the process of being launched in 2021

The goal of ECS Sensors Plus, as a one-stop shop journal for sensors, is to advance the fundamental science and understanding of sensors and detection technologies for efficient monitoring and control of industrial processes and the environment, and improving quality of life and human health.

*Nomination submission begins: May 18, 2021*



# Numerical investigation of the effects of hydrofoil vibrations on the unsteady behavior of cavitation

Linlin Geng, Jian Chen, Oscar De La Torre, and Xavier Escaler\*

Universitat Politècnica de Catalunya (UPC). Av. Diagonal 647, 08028 Barcelona, Spain.

E-mail: xavier.escaler@upc.edu

**Abstract.** In order to better understand the fluid-structure interaction (FSI) in hydraulic machines, this study aims to numerically investigate the flow around an oscillating hydrofoil with special attention on the effect of unsteadiness on leading edge cavitation. The cavitating flow has been modelled as incompressible with a Shear Stress Transport (SST) turbulence model coupled with a transition model, and with a mass transport equation between vapor and water. The sinusoidal motion of the hydrofoil has been implemented by using a moving mesh technique. The numerical results, which have been validated with experimental data, show that a critical frequency exists showing two different behaviors. For pitching frequencies above this critical frequency, the cavitation shedding frequency is linearly dependent on the pitching frequency. Moreover, this change of cavitation dynamics is explained by a pressure phase shift and an amplitude change observed as the pitching frequency increases.

## 1. Introduction

In hydraulic machines with a wicket gate, the non-uniform flow field at the guide vane outlet provokes a periodic fluctuation of the relative velocity angle of attack entering the blades [1]. This is a well-known phenomenon induced by the rotor-stator interaction (RSI) that generally affects Francis and Kaplan runner blades. For example, the RSI has been found to modulate the dynamic behavior of erosive blade cavitation. In addition, several investigations have demonstrated that the vibrations induced by RSI can lead to premature cracks in pump-turbines [2]. In order to understand the effects of RSI phenomena in hydraulic turbines, it is worth to study the influence of the flow unsteadiness on the cavitation dynamic behavior simulated around oscillating 2D hydrofoils. For example, it might be possible to develop strategies to actively control the cavity behavior by studying the relationships between the hydrofoil pitching frequency and the shedding frequency of the leading edge cavitation. Hence, potential ways to design safer and more reliable turbines and pump-turbines can be developed.

## 2. Experiment and numerical methods

### 2.1. Experiment description

The experiment taken as a reference was carried out at the cavitation tunnel of the Laboratory for Hydraulic Machinery in EPFL [3]. A hydrofoil, which has a NACA009-7.38 45/1.95 thickness distribution, a chord,  $c$ , of 100 mm and a span,  $b$ , of 150 mm, was mounted at the mid-height of the test section. The angle of attack was adjusted by a driving system which created hydrofoil angular pitching



oscillations at different frequencies. For the experiment being simulated, the hydrofoil was oscillating sinusoidally with a peak amplitude of  $1^\circ$  around a mean angle of attack of  $3^\circ$  as shown in figure 1. In addition, the inflow velocity,  $U_\infty$ , was 25 m/s, corresponding a Reynolds number of  $2.2 \times 10^6$ , the cavitation number,  $\sigma = (P_\infty - P_V)/0.5\rho_l U_\infty^2$ , was 1.15, where  $P_\infty$  and  $P_V$  are the pressure at the inlet and the vapor pressure, respectively, and  $\rho_l$  denotes the water density. Notice that when the experiment was conducted with fixed angles of attack under the above operating conditions the following observations were found:

- At  $2^\circ$ : no leading edge cavitation appears.
- At  $3^\circ$ : a small steady attached cavity develops from the leading edge.
- At  $4^\circ$ : an unsteady cloud cavitation appears with a shedding frequency around 210 Hz.

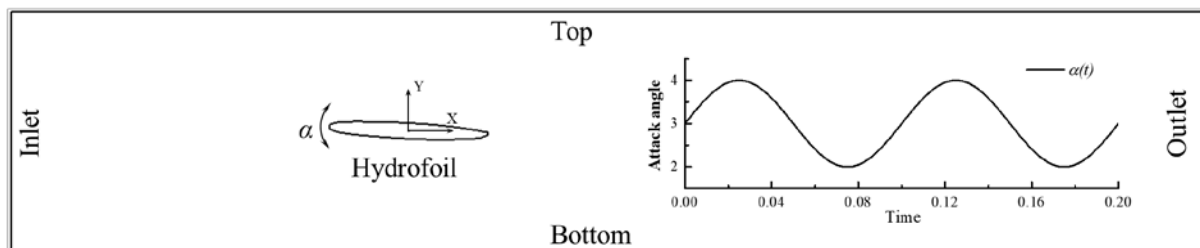


**Figure 1.** Experimental test section with named boundaries and the evolution of the angle of attack.

## 2.2. Numerical method

In the present numerical investigation, the multiphase URANS equations were considered as the governing system, and based on the homogeneous mixture assumption, the governing equations for the mixture quantities are given as follows:

$$\frac{\partial \rho_m}{\partial t} + \nabla \cdot (\rho_m u) = 0 \quad (1)$$

$$\frac{\partial (\rho_m u)}{\partial t} + \nabla \cdot (\rho_m uu) = -\nabla p + \nabla \cdot \left[ (\mu_m + \mu_t)(\nabla u + u\nabla - \frac{2}{3} \nabla \cdot u) \right] \quad (2)$$

where  $u$  and  $p$  are the mixture flow velocity and pressure,  $t$  is the time,  $\mu_t$  is the turbulent eddy viscosity and  $\mu_m$  and  $\rho_m$  are the mixture viscosity and the mixture density, respectively.

To simulate the unsteady cavitating flows around the pitching hydrofoil, three subsystems were considered to close the governing system of equations and to resolve them simultaneously. The first subsystem is the turbulence equation for computing  $\mu_t$ . In the present simulation, the  $k-\omega$  SST turbulence model coupled with a two-equation  $\gamma-Re_\theta$  transition model was used because it has the ability to well simulate the cavitating flows around pitching hydrofoils according to references [4, 5]. Besides, to overcome the overestimated turbulent viscosity predicted by the original eddy-viscosity equation, Reboud's density correction method was employed to reproduce the unsteady cavity behavior [6]. The second subsystem is the cavitation modelling using a transport equation with a source term built as the Zwart model to account for the mass transfer between the water and vapor. The third subsystem is the dynamic mesh method to reproduce the hydrofoil movement like in the experiment. The displacement diffusion model for mesh motion was used in which the mesh is treated as an elastic solid with variable stiffness and it is constrained to conform to the moving hydrofoil geometry, as well as to the other domain boundaries. As a result, the mesh elements near the hydrofoil move with the hydrofoil without too much distortion. However, the relatively larger mesh elements far away from the hydrofoil can be significantly distorted.

The numerical settings are summarized as follows. The inlet boundary setup was defined with the corresponding normal velocity equal to  $U_\infty$ , the average static pressure was specified at the outlet boundary according to the cavitation number. A no-slip wall condition was set for the top, bottom and

hydrofoil surfaces. On the two lateral faces of the fluid domain, a symmetry condition was setup to simulate a 2D flow. Moreover, the pressure-velocity direct coupling method was used to solve the governing equations. The high-resolution scheme was used for the convection terms. The second order implicit time scheme was used for the transient term. Several successive iterations were set within each physical time step. A very small residual criterion of  $10^{-5}$  and a large iterative number were set to march the solution towards convergence in every time step.

In addition, the simulation parameters were determined by conducting a sensitivity study comparing the numerical results obtained by doubling the grid size and by setting different time-steps. Based on that, a mesh with 65306 elements and a time step of 0.000025 s were finally selected. For the present simulation, hydrofoil pitching frequencies,  $f$ , of 10, 50, 100, 150, 200 and 250 Hz were chosen to explore the relation between the cavity behavior and the hydrofoil oscillation.

### 3. Results and discussions

The numerical results were firstly validated by comparison with the available experiment data. Then, the influence of pitching frequency on the cavitation dynamic behavior and on the hydrofoil performance was analyzed.

#### 3.1. Numerical validation

For validation purposes, simulations with a fixed angle of attack were carried out firstly and it was confirmed that the numerical results reproduced a similar behaviour as the one observed in the experiment. In particular, leading edge cavitation does not appear at a fixed angle of  $2^\circ$ , while it appears at  $3^\circ$ . And at  $4^\circ$ , the cavity becomes unsteady with a shedding frequency of 240 Hz which is close to the experimental observations. Figure 2 compares the experimentally measured and the numerically predicted time histories of the pressure coefficient,  $C_p$ , over one oscillation period,  $T_{ref} = 1/f$ , at position  $x/c = 0.325$ , and the corresponding time-frequency results when the pitching frequency  $f$  is 10 Hz. It can be observed that both simulation and experiment show the fluctuations of  $C_p$  with similar trends and amplitude variations.  $C_p$  starts to fluctuate at the beginning of the hydrofoil oscillation and then develops a highly periodic pulsation which corresponds to the attached cavity growth and shedding process. When the angle of attack decreases from  $3^\circ$  to  $2^\circ$  and the cavity disappears,  $C_p$  stabilizes. However, comparing the measured and predicted time signals from  $T/T_{ref} = 0.15$  to 0.4, it can be seen that the simulation underestimates the frequency of the pressure fluctuations.

In general, these similarities prove that the present numerical method is able to predict the expected cavity behavior around the pitching hydrofoil. Consequently, we assumed that this model can be used to analyze the influence of the hydrofoil pitching frequency on the cavitation dynamic behavior.

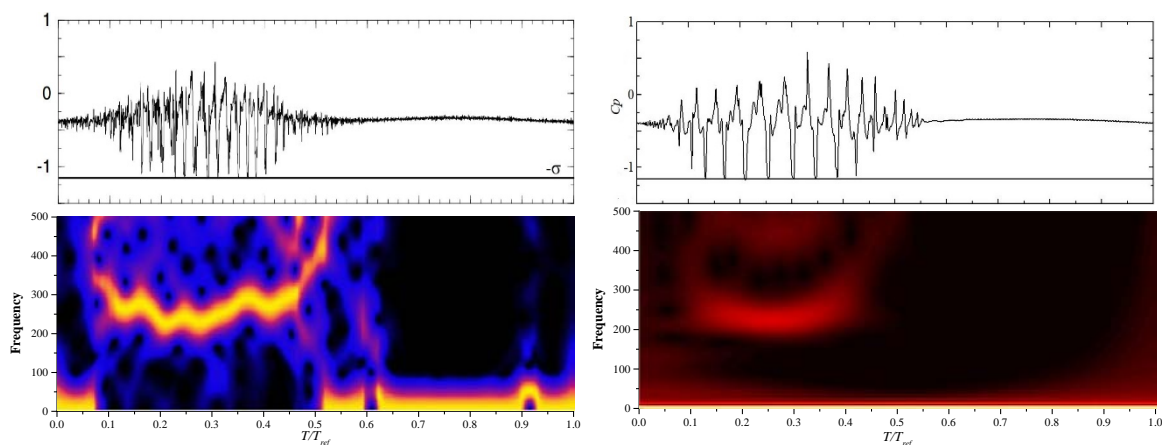


**Figure 2.** Comparison between the experimental (left) and numerical (right) results of the pressure coefficient time evolution and corresponding time-frequency plots. Experimental results were taken from [3].

### 3.2. The influence of pitching frequency

The numerical results show that the cavitation dynamic behavior is significantly influenced by the change of pitching frequency  $f$ . It can be seen from figure 3 that the maximum cavity length decreases with increasing values of  $f$ , especially for pitching frequencies below 100 Hz. In addition, figure 4 shows the time history of the pressure at location  $x/c = 0.325$  over a time duration of 0.1 s. Notice that the instants with the lowest pressures represent the cloud shedding because the amplitude of pressure drops to minimum values when the cloud flows over the location of the numerical sensor. As expected, the shedding process is mainly concentrated on the first half of the pitching period for the pitching frequency of 10Hz, i.e. when the angle of attack is larger than  $3^\circ$ .

To study the cavity behavior under different pitching frequencies, an equivalent shedding frequency,  $f_{equ} = N/T_{ref}$ , is defined where  $N$  is the number of shed clouds during one period of hydrofoil oscillation,  $T_{ref}$ . From figure 4, we can count values of  $N = 11$  and 2 for pitching frequencies  $f = 10$  and 50 Hz, respectively, and of  $N = 1$  for  $f \geq 100$  Hz. Hence,  $f_{equ}$  has been plotted with a black line in figure 5 as a function of  $f$ , and correspondingly, the value of  $N$  has also been plotted with a blue line. It can be seen that there seems to be a critical frequency,  $f_c$ , which separates two different behaviors:

- Behavior 1 when  $f < f_c$ : the equivalent frequency does not linearly depend on the pitching frequency.
- Behavior 2 when  $f > f_c$ , the equivalent frequency increases linearly and is equal to the pitching frequency.

Here, notice that we do not have enough precision to ensure that  $f_c$  is exactly 100 Hz since we lack results for pitching frequencies between 50 and 100 Hz.

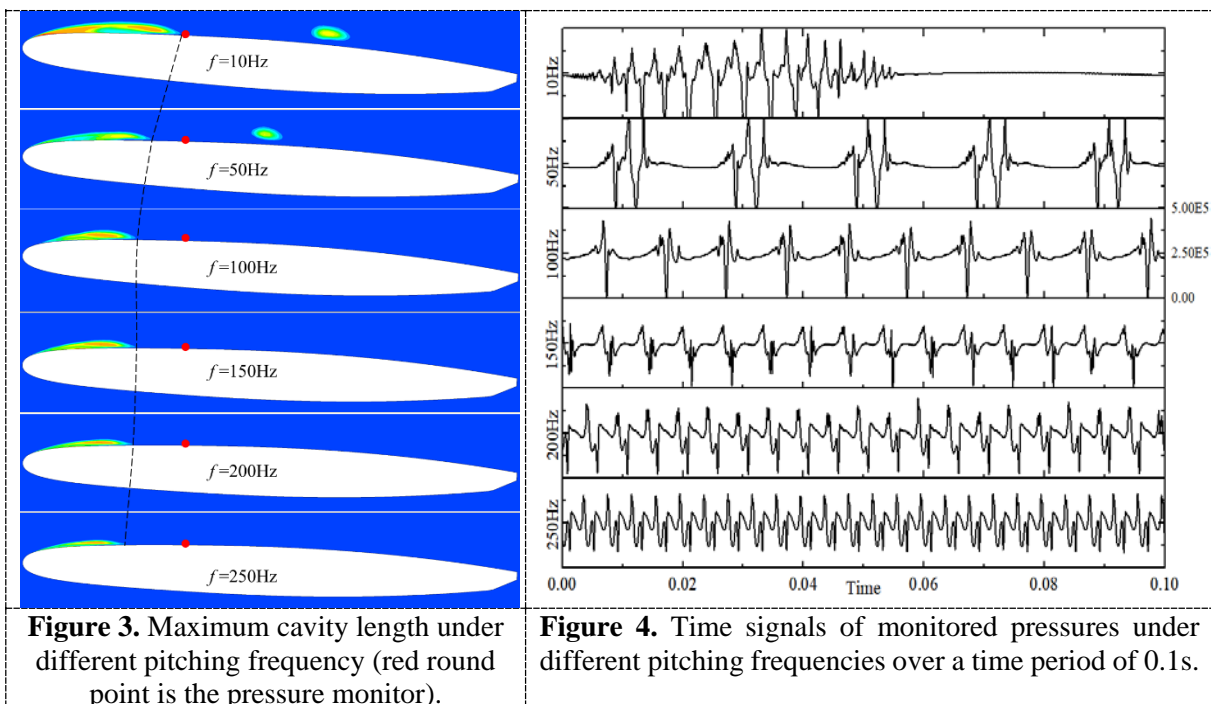


**Figure 3.** Maximum cavity length under different pitching frequency (red round point is the pressure monitor).

**Figure 4.** Time signals of monitored pressures under different pitching frequencies over a time period of 0.1s.

In addition, figure 6 shows the normalized time at which the cavity reaches its maximum length for different pitching frequencies with red dots over the time evolution of the hydrofoil angle of attack during one oscillation. It can be seen that the appearance of red points is delayed for  $f \geq 100$  Hz, even though the maximum cavity length becomes shorter in these cases. However, the instant of cavity inception is similar for any pitching frequency, which indicates that the time duration with the cavity attached on the hydrofoil is longer as the  $f$  increases. For example, for  $f = 100$ Hz, the normalized time needed for cavity growth from inception to its maximum length is about one half of a period, while it is

about three fourths of a period for  $f = 250$  Hz. Thus, the evolution of cavity behavior including cavity growth, detachment and shedding changes with the change of  $f$ . To understand this phenomenon, the single phase flow without cavitation around the pitching hydrofoil was simulated and compared at different pitching frequencies. Figure 7 shows the time histories over one period of the pressures at two different positions  $x/c = 0.2$  and  $0.3$  on the hydrofoil suction side. It is obvious that the pressures fluctuate with larger amplitudes when  $f$  increases. At  $x/c = 0.2$ , the pressure fluctuates from 180000 to 240000 Pa for  $f = 10$  Hz, while it fluctuates from less than 160000 to more than 260000 Pa for  $f = 250$  Hz. And these increases are even larger for the pressure at  $x/c = 0.3$ . Besides, a clear phase shift is found out as  $f$  increases. For example at  $x/c = 0.2$  and for  $f = 10$  Hz, the minimum pressure almost is achieved at  $T/T_{ref} = 0.25$ , corresponding to the maximum angle of attack. However, for  $f > 100$  Hz, the minimum pressure is advanced and it appears at around  $T/T_{ref} = 0.125$ . Moreover, these differences are even more evident for the pressure signals at  $x/c = 0.3$ . In summary, these observations are linked to the observed cavitation dynamic behavior.

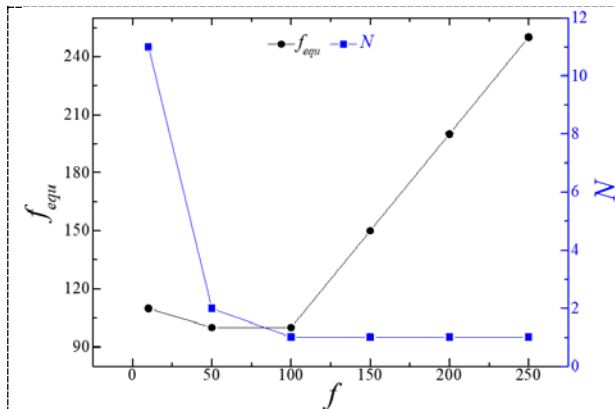


**Figure 5.** Equivalent frequency,  $f_{equ}$ , and number of shed cloud,  $N$ , as a function of pitching frequency,  $f$ .

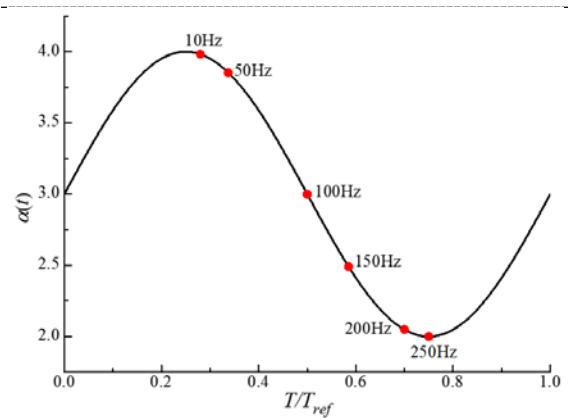


**Figure 6.** Normalized instants marked with red dots at which the attached cavity reaches its maximum length for different pitching frequencies.

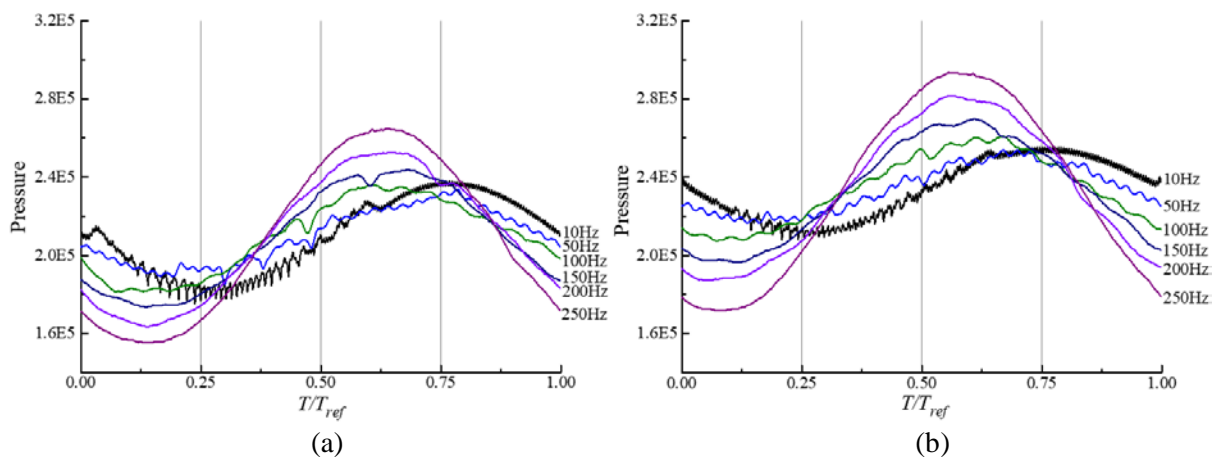


**Figure 7.** Pressure evolution over one cycle under different pitching frequencies at  $x/c = 0.2$  (a) and  $0.3$  (b).

#### 4. Conclusion

In the present investigation, the unsteady cavitating flow around a pitching hydrofoil has been numerically investigated with emphasis on the influence of the pitching frequency on the main cavity

fluctuation. The numerical model was preliminary validated with available experimental data. According to the numerical results, a critical pitching frequency has been found that separates two regions with different cavity dynamic behaviors. For higher frequencies, the cavity fluctuation is dominated by the pitching frequency and the normalized time needed for cavity growth is longer. As the pitching frequency increases, a phase shift and an amplitude change on the suction side pressure is also predicted that is linked to the change of cavity behavior.

### References

- [1] Zobeiri A, Kueny JL, Farhat M, Avellan F 2006 Pump-turbine rotor-stator interactions in generating mode: pressure fluctuation in distributor channel. *In Proc. of the 23rd IAHR Symp (Yokohama, Japan)* Vol. 1, No. CONF, pp. 1-10.
- [2] Münch C, Ausoni P, Braun O, Farhat M, and Avellan F 2010 Fluid–structure coupling for an oscillating hydrofoil. *J. Fluids Struct*, 26(6), 1018-1033.
- [3] Caron JF 2002 Etude de l'influence des instationnarités des écoulements sur le développement de la cavitation. *No. THESIS*. EPFL.
- [4] Huang B, Ducoin A, Young YL 2013 Physical and numerical investigation of cavitating flows around a pitching hydrofoil. *Phys. Fluids*, 25(10), 102109..
- [5] Ducoin A, Astolfi JA, Deniset F, Sigrist JF 2009 Computational and experimental investigation of flow over a transient pitching hydrofoil. *Eur. J. Mech. - B/Fluids*, 28(6), 728-743.
- [6] Geng L, Escaler X 2020 Assessment of RANS turbulence models and Zwart cavitation model empirical coefficients for the simulation of unsteady cloud cavitation. *Eng. Appl. Comp. Fluid Mech*. 14(1), 151-167.

### Acknowledgments

This project has received funding from the European Union's Horizon 2020 research and innovation programme under grant agreement No 814958, and from China Scholarship Council.